

Oxygen Production and Numerical Simulations of the Interphase Transport in the Modified Oscillating Briggs–Rauscher Reaction

Peter Ševčík,* Katarína Kissimonová, and L'ubica Adamčíková

Department of Physical Chemistry, Comenius University, 842 15 Bratislava, Slovak Republic

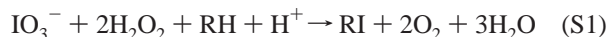
Received: May 28, 2002; In Final Form: November 15, 2002

The volume of gaseous oxygen produced during the Briggs–Rauscher (BR) oscillating reaction with acetone was measured. The rates of oscillatory oxygen evolution were calculated and the effects of stirring rate and addition of acrylamide on the oscillations were studied. The dynamic behavior of the modified BR reaction was modeled by mechanisms suggested by Noyes and Furrow (*J. Am. Chem. Soc.* **1982**, *104*, 45) and De Kepper and Epstein (*J. Am. Chem. Soc.* **1982**, *104*, 49), supplemented by the physical processes of the iodine and oxygen interphase transport. The calculated oscillatory parameters are in satisfactory agreement with experiment.

Introduction

The Briggs–Rauscher (BR) reaction, discovered in 1973,¹ is among the most impressive oscillating reactions, and it is very convenient for the demonstration of nonlinear chemical dynamics.² The classical BR reaction system includes malonic acid, Mn(II) ions [which are components of the Belousov–Zhabotinsky (BZ) oscillating reaction], hydrogen peroxide, and iodate ions [which are components of the Bray–Liebhafsky (BL) oscillating reaction] in acidic solution. If starch is used as an indicator for enhancing the color due to iodine, the oscillations usually persist for only about 10 min in a closed system and follow the color sequence from colorless to yellow to deep blue before repeating with a frequency of several cycles per minute. The potential of an iodide-selective electrode behaves very similarly, and oscillations in the concentration of iodide ions can be observed.

The overall stoichiometric change is suggested to be³



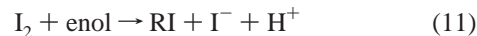
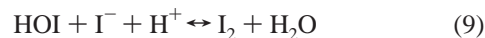
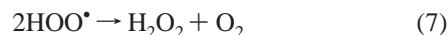
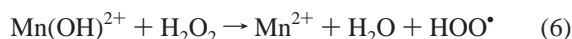
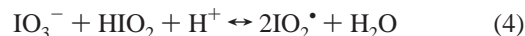
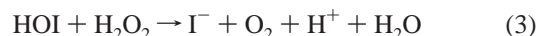
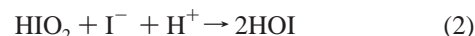
This change can be generated by two stoichiometric processes designated S2 and S3



where $\text{RH} = \text{CH}_2(\text{COOH})_2$ and $\text{RI} = \text{CHI}(\text{COOH})_2$. If Mn(II) is also present, the same process (S2) can also take place much more quickly.

In 1982, two groups independently proposed a skeleton mechanism for the classical BR reaction that could lead to oscillations in batch or continuously stirred tank reactor (CSTR) mode. Noyes and Furrow (NF)⁴ deduced their mechanism from studies of subsystems, and De Kepper and Epstein (DE)⁵ formulated a nearly identical mechanism from CSTR studies.

The following 11 pseudoelementary reactions are sufficient to explain oscillations in the classical batch BR system⁴



Cook⁶ found that various substitutions could be made in the classical BR reaction and still maintain oscillations. For instance, malonic acid can be replaced by acetone. The behaviors of these two substrates are different as a result of greater oxidation of organic material in the malonic acid system, but the underlying mechanisms seem to be closely related.⁷

The effects of macromixing and stirring on the photoinduced phase transition in the batch-mode classical BR reaction with malonic acid were examined both experimentally and theoretically.^{8,9} The course of the reaction was followed spectrophotometrically by monitoring of the iodine concentration and potentiometrically with iodide-selective and Pt redox electrodes. Vanag et al.^{8,9} deduced that these effects are due to the influence

of stirring on microheterogeneities and suggested the existence of effects of internal fluctuations on the dynamics of complex nonlinear chemical systems.

The classical BR reaction is also photosensitive, and oscillations can stop under strong illumination. Kumpinsky et al.¹⁰ performed calculations to model irradiation in a CSTR. They supplemented the BR mechanism by additional steps involving the photogeneration and subsequent reactions of iodine atoms. The calculations showed qualitative agreement with some experimentally observed phenomena. Vukojević, Sørensen, and Hynne¹¹ presented a more detailed mechanism for the classical BR reaction that well simulates a wide range of experimental results for open reactors, in particular quenching effects. This mechanism contains common fundamental steps from the NF and DE models. The effects of the addition of halide ions on the oscillatory regime in the classical BR reaction have also been studied.^{12,13} The addition of bromide ions to an active oscillating BR reaction causes a rapid suppression of the oscillations.¹³ Inhibitory effects of the addition of aqueous extracts of soy flour to an active BR mixture were recently reported.¹⁴

Spatial patterns in the classical BR reaction resemble in many respects those described in the well-known Belousov–Zhabotinsky reaction, but Müller et al.¹⁵ also observed unusual behavior in some diffusion-dependent processes, for example when waves are moving across gas bubbles or during wave collision.

The substitution of acetone for malonic acid has at least two advantages. First, the oscillatory parameters are changed. The period of oscillations is increased to several minutes, and the oscillations in the rate of oxygen production can be followed relatively easily, as described in our earlier paper¹⁶ concerning the Bray–Liebhafsky reaction. Second, the evolution of CO₂, which might be a gaseous product in the case of malonic acid and which is not included in the models, is ruled out for acetone.

Therefore, in this work, the time dependence of the volume of produced gaseous oxygen in the BR reaction with acetone is reported. We were able to calculate the rates of oxygen evolution and to study the effects of the stirring rate on the rate of oxygen production and on the oscillations in the BR reaction. In our earlier papers on the BL reaction,^{16,17} we showed that the rate of interphase transport of I₂ and O₂ can be greatly influenced by stirring and that such physical processes can inhibit oscillations.

The other aim of this work was to test the possibility of modeling the effects of interphase transport for iodine and oxygen in the modified BR reaction. The NF model (reactions 1–11, but with RH = acetone) was supplemented with the physical processes of iodine and oxygen interphase transport



The results of numerical simulations are compared to experimental results on oxygen production in the modified BR reaction.

Experimental Section

Materials and Methods. Freshly prepared solutions of common reagent-grade chemicals and redistilled, deionized water were used. Solutions of H₂O₂ were made from 30% aqueous material without stabilizer obtained from Merck. The following initial reactant concentrations were used: 0.035 M

KIO₃, 0.4 M H₂O₂, 1.3 M (CH₃)₂CO, 0.005 M MnSO₄, and 0.1 M H₂SO₄. The experiments were carried out in a well thermostated (25.0 ± 0.1 °C) cylindrical glass reaction vessel (diameter 3.5 cm, height 7.2 cm) in the dark. The volume of the reaction mixture was 40 mL with a free surface area above it that varied from 7.98 to 9.62 cm² depending on experimental setup. The lower value corresponds to the experiments when a commercial platinum indicator macroelectrode and a reference mercury sulfate electrode were inserted into the reaction solution. The higher value was calculated for experiments performed without inserted electrodes when only the oxygen evolution was monitored. There were also two other holes in the stopper. One was for a glass capillary tube (diameter of 0.3 cm in the stopper, but 0.1 cm at the end) immersed into the reaction solution, through which O₂ gas from an oxygen pressure vessel was bubbled into the reaction solution to reach saturation before the BR reaction was started. The second hole was for a glass tube (diameter 0.5 cm), which was connected via tubing to a 250-mL closed Erlenmeyer-like flask reservoir containing 220 mL of water placed above the level of the reaction vessel. The details of our experimental arrangement for measuring the production of oxygen in the BL system were designed in our previous work.¹⁶

An analogous procedure for monitoring the evolution gaseous oxygen was used in our modified BR system. Oxygen saturation of both the BR reaction mixture and the water reservoir at 101.3 kPa before the reaction was started was reached by oxygen bubbling (600 mL min⁻¹) from the pressure vessel for at least 10 min. Then, bubbling was stopped, and the entire amount of oxygen evolved during the BR reaction was allowed to enter into the oxygen-saturated water reservoir and accumulate only in the space above the water. The Erlenmeyer flask reservoir was equipped with a tap at the bottom, which, when opened, enabled the outflow of water. It was verified that, in this experimental arrangement, the volume of water replaced corresponds to the volume of oxygen produced. The time dependence of the exact volume of water flowing out was measured point-by-point by reading the water level in a calibrated buret. In comparison to ref 16, the only useful difference was that we were able to read the exact volume as often as we wished, because we had available a special sport stopwatch with data memory.

The reactant solutions were added into the reaction vessel in the order aqueous solution of H₂SO₄, KIO₃, H₂O₂, and acetone, and finally, a small amount of MnSO₄ (saturated by oxygen) was quickly added, after which the oscillation reaction was started. In the experiments with the addition of acrylamide, it was verified that there was no observable chemical reaction between acrylamide and any of the reactants under given conditions for 120 min. The reaction solution was stirred magnetically with a Teflon-coated stirrer (polygon-shaped, 2 cm × 0.8 cm). The stirring rate of the magnetic stirrer was kept constant at a value between 50 and 1000 rpm. For comparison, several blank experiments were performed to determine whether any evaporation of acetone at various stirring rates could affect the results. We measured both the volume of displaced water and the decrease in the volume of the reaction mixture without H₂O₂ in the reaction vessel. We found a maximal loss of 0.03% in acetone concentration at 1000 rpm after 120 min.

Oscillations in the BR mixture were also followed potentiometrically by recording the time dependence of changes in the platinum redox potential using a Radelkis OH-105 polarograph.

Simulations. Computer simulations were carried out on a PC Pentium II 400-MHz computer (using a Linux operating

TABLE 1: Rate Constants Used in Simulations for the Modified BR Reaction

reaction	rate	rate constant
R1	$k_1[\text{IO}_3^-][\text{I}^-][\text{H}^+]^2$	$k_1 = 1.4 \times 10^3 \text{ M}^{-3} \text{ s}^{-1}$
R2	$k_2[\text{HIO}_2][\text{I}^-][\text{H}^+]$	$k_2 = 2.0 \times 10^9 \text{ M}^{-2} \text{ s}^{-1}$
R3	$k_3[\text{H}_2\text{O}_2][\text{HOI}]$	$k_3 = 37.0 \text{ M}^{-1} \text{ s}^{-1}$
R4	$k_4[\text{HIO}_2][\text{IO}_3^-][\text{H}^+]$	$k_4 = 1.516 \times 10^4 \text{ M}^{-2} \text{ s}^{-1}$
R-4	$k_{-4}[\text{IO}_2]^2$	$k_{-4} = 1.607 \times 10^9 \text{ M}^{-1} \text{ s}^{-1}$
R5	$k_5[\text{IO}_2^*][\text{Mn}^{2+}]$	$k_5 = 1.0 \times 10^4 \text{ M}^{-1} \text{ s}^{-1}$
R6	$k_6[\text{Mn}(\text{OH})^{2+}][\text{H}_2\text{O}_2]$	$k_6 = 3.2 \times 10^4 \text{ M}^{-1} \text{ s}^{-1}$
R7	$k_7[\text{HOO}^*]^2$	$k_7 = 7.5 \times 10^5 \text{ M}^{-1} \text{ s}^{-1}$
R8	$k_8[\text{HIO}_2]^2$	$k_8 = 45.3 \text{ M}^{-1} \text{ s}^{-1}$
R9	$k_9[\text{H}^+][\text{HOI}][\text{I}^-]$	$k_9 = 3.1 \times 10^{12} \text{ M}^{-2} \text{ s}^{-1}$
R-9	$k_{-9}[\text{I}_2]$	$k_{-9} = 2.2 \text{ s}^{-1}$
R10	$k_{10}[(\text{CH}_3)_2\text{CO}]$	$k_{10} = 4.0 \times 10^{-6} \text{ s}^{-1}$
R-10	$k_{-10}[\text{enol}]$	$k_{-10} = 14.0 \text{ s}^{-1}$
R11	$k_{11}[\text{enol}][\text{I}_2]$	$k_{11} = 9.1 \times 10^5 \text{ M}^{-1} \text{ s}^{-1}$
R12	$k_{12}[\text{I}_{2(\text{aq})}]$	$k_{12} = \text{parameter}$
R13	$k_{13}[\text{O}_{2(\text{aq})}]$	$k_{13} = \text{parameter}$

system) by means of numerical integration of a differential equation system derived from the model under study. We used the modified NF mechanism with acetone supplemented by the processes in eqs 12 and 13. The corresponding rate equations and rate constants are shown in Table 1. $[\text{I}_{2(\text{aq})}]$ and $[\text{O}_{2(\text{aq})}]$ represent the concentrations of dissolved iodine and oxygen, respectively, that were formed chemically during the BR reaction. The concentrations of I^- , HIO , HIO_2 , $\text{I}_{2(\text{aq})}$, IO_3^- , $\text{O}_{2(\text{aq})}$, H_2O_2 , IO_2^* , Mn^{2+} , MnOH^{2+} , HOO^* , $(\text{CH}_3)_2\text{CO}$, and $\text{CH}_2=\text{C}(\text{OH})\text{CH}_3$ were set as variables. Calculations were performed using the Fortran subroutine LSODE from a systematized collection of ODE solvers, ODEPACK,¹⁸ with an absolute error tolerance of 10^{-30} and a relative error tolerance of 10^{-6} . The initial concentration values of all species not considered to be present at the beginning were set to 0.

Results and Discussion

Oxygen Production. First, we tried to measure the oxygen evolution in the BR system if experiments were conducted without any electrodes inserted into the BR reaction solution. For comparison, changes in the potential of the Pt redox electrode were simultaneously measured in another set of experiments. Only minor changes in oscillatory behavior were observed.

We can conclude that electrodes inserted into the reaction vessel have no observable influence on the oxygen production at sufficient stirring rates and that a large Pt electrode surface does not facilitate the gas evolution by providing more nucleation sites.

Figure 1 represents a typical experiment and shows the time dependence of the volume of oxygen produced (curve 1a) and the rate of O_2 evolution (curve 1b, calculated from curve 1a) during the BR reaction at 100 rpm. The reaction begins without an induction period (IP), and the period of oscillations (PO) gradually decreases from $\text{PO}_1 = 6.3$ min to $\text{PO}_2 = 5.5$ min, $\text{PO}_3 = 5.0$ min, and furthermore. Both the volume of oxygen evolved (VO) and amplitudes of oscillations (AO) also decrease in successive steps (with $\text{VO}_1 = 11.8$ mL and $\text{AO}_1 = 4.6$ mL min^{-1}). The number of oscillations ranged from 45 to 48. The BR oscillations lasted for roughly 102–113 min. The total volume of oxygen produced was 133–134 mL at 25 °C and 101.3 kPa.

In contrast to the effect of stirring on the batch BL oscillating reaction,^{16,19–21} in which rapid stirring suppresses oscillations and the escape rate of oxygen from the solution should be taken into account in the modeling of the BL oscillations, the effect

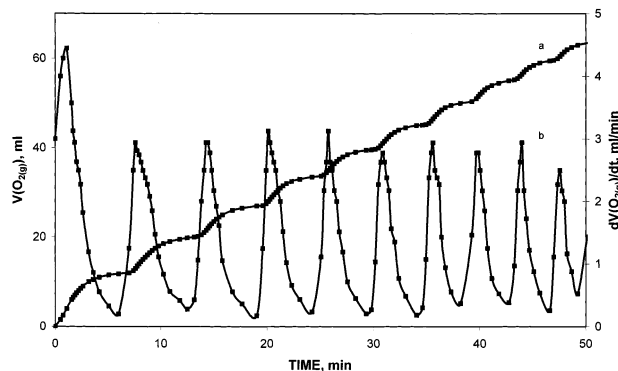


Figure 1. Time dependence of (a) the oxygen volume produced and (b) the rate of oxygen evolution in the modified Briggs–Rauscher reaction at 100 rpm and 25 °C. The BR solution initially contained 0.035 M IO_3^- , 0.1 M H_2SO_4 , 1.3 M acetone, 0.4 M H_2O_2 , and 0.005 M Mn^{2+} .

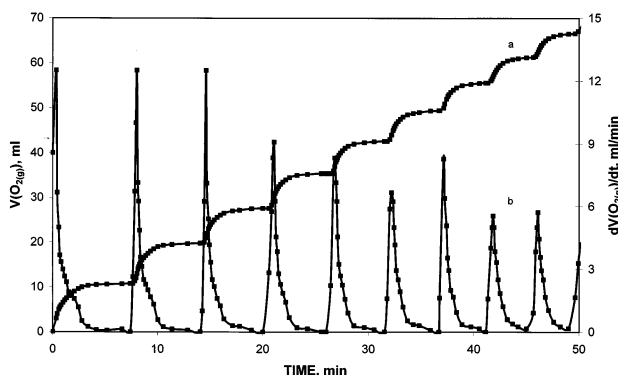


Figure 2. (a) Volume of oxygen evolved and (b) rate of O_2 evolution in the BR reaction at 1000 rpm. Other constraints are as in Figure 1.

of stirring on the modified BR reaction with acetone is not as expressive and seems to be closer to that in the classical BR reaction with malonic acid. Vanag et al.⁸ observed that, with increasing stirring intensity, the oscillation amplitude and the duration of the oscillatory state increase by about 100 and 15–20%, respectively, for the classical batch BR reaction.

In our setup, an increase of the stirring rate to 1000 rpm does not stop the oscillations (Figure 2). PO_1 is increased to 7.5 min, PO_2 to 6.8 min, and PO_3 to 5.9 min. However, the number of oscillations decreases to 40–42, so that both the duration of oscillations and the volume of oxygen produced remain the same as at 100 rpm. It is noteworthy that the shape of the oscillations is different. The period when no oxygen bubbles are observed is lengthened, and the maximal AO is increased to 12.9 mL min^{-1} .

The detailed relationship of the Pt potential and the rate of oxygen evolved during one oscillation is shown in Figure 3. We can see that the positive Pt potential suddenly rises (curve 3a). The maximum in O_2 rate evolved (curve 3b) is reached at about the same time as the Pt potential is maximal. This delay is dependent on the rate of stirring. We found a delay of 9 s at 1000 rpm but 21 s at 100 rpm.

The rate of iodine production in the classical BR reaction is affected by the addition of acrylamide.²² We were able to demonstrate that the addition of acrylamide can change the oscillatory behavior of the BR reaction modified with acetone by following it both volumetrically and potentiometrically (Figure 4) as well. We can see that the duration of oscillations decreases to 73 min and the number of oscillations to one-half of its initial value. The total volume of oxygen produced during oscillatory period decreased from 134 to 118 mL for 1×10^{-3}

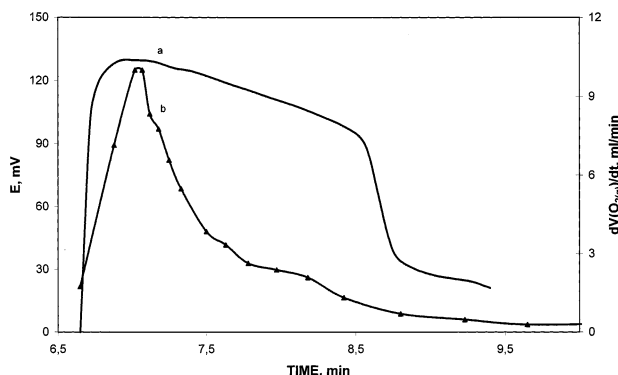


Figure 3. Detailed shape of the single BR oscillation at 1000 rpm: (a) Pt redox potential, (b) rate of O₂ evolution. Other constraints are as in Figure 1.

M acrylamide. Steps 3 and 7 involve reactions that lead to the direct formation of O₂. The addition of acrylamide, active as scavenger of HOO• radicals, might interfere with reaction 7. However, acrylamide can probably undergo other reactions, such as iodination by HOI.

Simulations. The set of NF⁴ reactions 1–11 is sufficient for simulations of the rate of the oxygen production in the modified BR reaction. However, the rate of interphase transport of iodine and oxygen can be influenced by the stirring rate. To model the effects of such interphase transport, we supplemented the NF mechanism by physical processes 12 and 13 with the rate equations shown in Table 1. The rate constants for iodine and oxygen removal were adjusted to be comparable to those used in the simulations of the BL reaction,^{20,23} in which the Schmitz and Kolar-Anić model^{24,25} was also supplemented by the physical processes of iodine and oxygen interphase transport. The entire model in eqs 1–13 shows a strong sensitivity to the parameters k_{12} and k_{13} . The replacement of malonic acid by acetone required that appropriate rate constants be used for reactions 10 and 11.

A simulation of the effect of iodine interphase transport on the calculated hypothetical concentration of dissolved oxygen in the BR solution for $k_{13} = 0$ is shown in Figure 5. When no oxygen gas evolution is allowed in the model, the concentration of the dissolved oxygen increases step-by-step with time depending on the value of the rate constant for iodine removal. Trace 5a is a reference curve calculated for a system without the physical removal of either iodine or oxygen. The rates of escape of I₂ molecules from a standard solution of I₂ to the

gaseous phase above the liquid solution caused by different stirring rates in the same reaction vessel were determined spectrophotometrically and were described in our earlier work.¹⁷ Curve 5b is designed for $k_{12} = 2.74 \times 10^{-4} \text{ s}^{-1}$, which corresponds to a stirring rate of 100 rpm in our experimental arrangement. The calculated final concentration of O₂ in the reaction solution can achieve a value of 0.069 M for $k_{12} = 0 \text{ s}^{-1}$ and 0.084 M for $k_{12} = 3.33 \times 10^{-2} \text{ s}^{-1}$ when oscillations are completely suppressed (curve 5d). Noyes, Bowers, and co-workers^{26–28} found that the apparent critical supersaturations of dissolved oxygen were in the range 0.04–0.06 M at 35 °C; a maximum dissolved oxygen concentration of about 0.12 M was found at 25 °C and 101.3 kPa. The equilibrium solubility of oxygen is 0.001 26 M under the same conditions.²⁷ Of course, supersaturation can easily be removed by rapid stirring. Sufficiently rapid stirring simultaneously greatly increases the rate of transport of iodine from the BR solution. In Figure 5c, which represents $k_{12} = 3.33 \times 10^{-3} \text{ s}^{-1}$ and corresponds to a rate of stirring of much more than 1000 rpm, we can see periodical evolution of oxygen, whereas oxygen supersaturation in the real BR system is very implausible.

Assuming ideal gas behavior, we can easily simulate the time dependence of the volume of gaseous oxygen for comparison with experiments. A simulation of the time dependence of the volume of gaseous oxygen evolved for the constant value $k_{12} = 4.14 \times 10^{-4} \text{ s}^{-1}$ that corresponds to a stirring rate of 1000 rpm is shown in Figure 6. A nonmonotonic increase can be observed for k_{13} varied from $8.33 \times 10^{-4} \text{ s}^{-1}$ (curve 6a) to $8.33 \times 10^{-2} \text{ s}^{-1}$ (curve 6c).

Relatively good agreement with experiments was obtained in the induction period (no IP) and the volume of oxygen evolved ($VO_1 \approx 10 \text{ mL}$ for $k_{13} = 8.33 \times 10^{-3} \text{ s}^{-1}$). Also, the diminishing period of oscillations is in accordance with the trend observed experimentally, although the calculated value of $PO_1 = 17.5 \text{ min}$ is greater. Furthermore, the number of oscillations (15) and the duration of oscillatory behavior (164 min) for $k_{13} > 8 \times 10^{-3} \text{ s}^{-1}$ differ quantitatively.

Figure 7 illustrates the typical oscillations in the rate of gaseous oxygen production in the BR reaction calculated for $k_{12} = 4.14 \times 10^{-4} \text{ s}^{-1}$ corresponding to a rate of stirring of about 1000 rpm. Traces 7a and 7b represent oscillations achieved for $k_{13} = 8.33 \times 10^{-2}$ and $8.33 \times 10^{-3} \text{ s}^{-1}$, respectively. The change in the value of k_{13} has no influence on the periods and number of oscillations. The simulated amplitude of oscillations

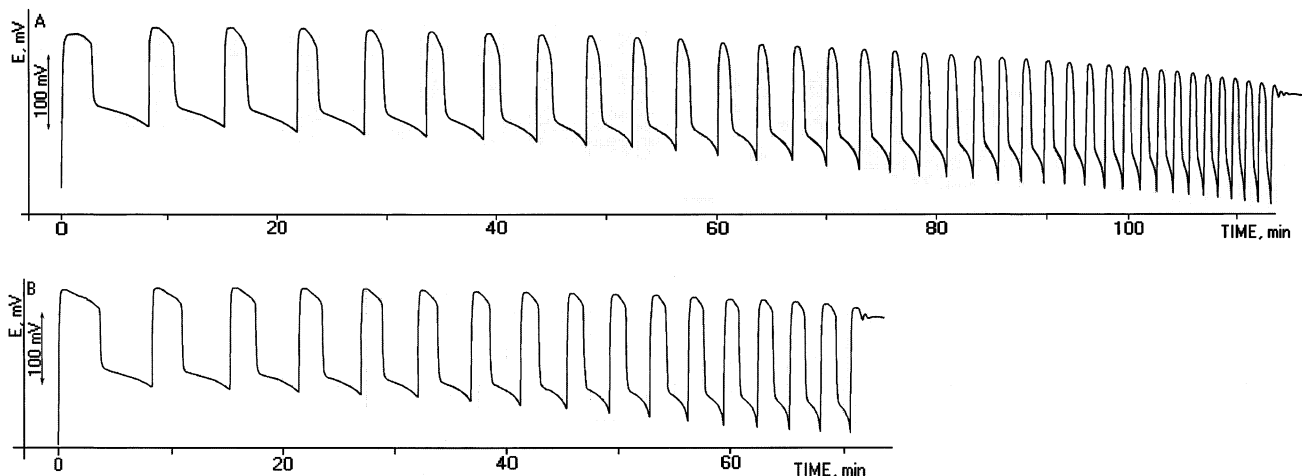


Figure 4. Recording of the Pt redox potential vs time at 100 rpm. (a) Reference mixture, initial conditions as in Figure 1. (b) Effect of the addition of 0.001 M acrylamide.

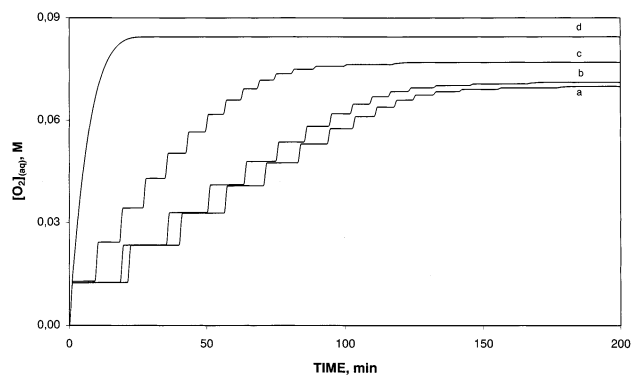


Figure 5. Simulation of the effect of iodine interphase transport on the dissolved oxygen concentration produced in the BR reaction. The initial concentrations are 0.035 M IO_3^- , 0.1 M H_2SO_4 , 1.3 M acetone, 0.4 M H_2O_2 , 0.005 M Mn^{2+} . Model reactions R1–R13, rate constants as in Table 1 with $k_{13} = 0$ and $k_{12} =$ (a) 0, (b) 2.74×10^{-4} , (c) 3.33×10^{-3} , and (d) $3.33 \times 10^{-2} \text{ s}^{-1}$.

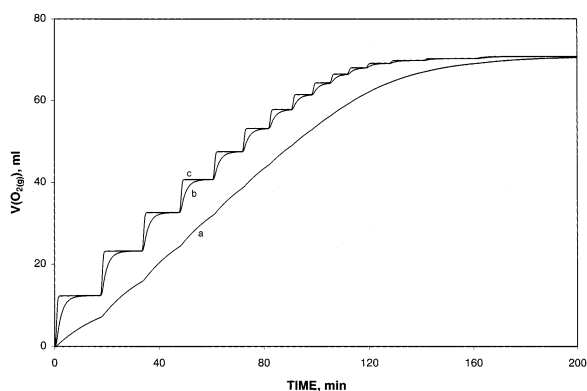


Figure 6. Simulated effect of the oxygen interphase transport on the volume of gaseous oxygen produced in the BR reaction. The initial concentrations are the same as in Figure 5, $k_{12} = 4.14 \times 10^{-4} \text{ s}^{-1}$, and $k_{13} =$ (a) 8.33×10^{-4} , (b) 8.33×10^{-3} , and (c) $8.33 \times 10^{-2} \text{ s}^{-1}$.

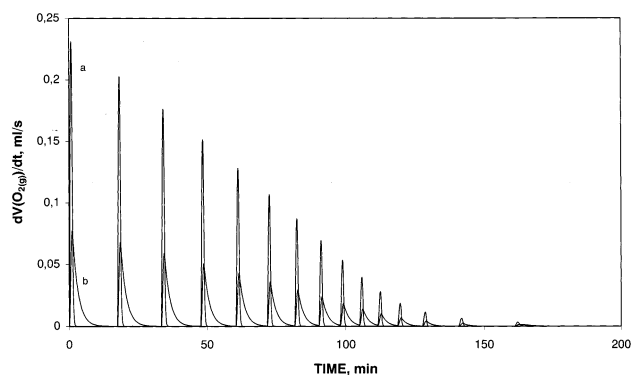


Figure 7. Simulations of the oxygen interphase transport effect on the rate of gaseous oxygen produced in the modified BR reaction. The model and initial concentrations are the same as in Figure 5, $k_{12} = 4.14 \times 10^{-4} \text{ s}^{-1}$, and $k_{13} =$ (a) 8.33×10^{-2} and (b) $8.33 \times 10^{-3} \text{ s}^{-1}$.

$\text{AO}_1 = 13.6 \text{ mL min}^{-1}$ for a value of $k_{13} = 8.33 \times 10^{-2} \text{ s}^{-1}$ is in very good agreement with AO_1 observed experimentally (Figure 2).

Simulations reveal that probably both the NF and DE models reflect the experimental findings. However, the exact value of the rate constants of iodine and oxygen transport can only be estimated for the real BR system, in which a great number of oxygen bubbles are formed and escape from the solution to the space above it. This effect might accelerate the vaporization of

I_2 molecules. Taking into consideration the measured value of the rate of O_2 transport between gas phase and solution in the BZ reaction,²⁹ which is dependent on the stirring rate, and refs 30 and 31, a value on the order ca. 10^{-4} s^{-1} can be expected in our experimental setup. This value of the rate constant corresponds to a mass-transfer coefficient of ca. $10^{-3} \text{ cm s}^{-1}$. To obtain good agreement with experimental results, we used in our simulations a higher value for k_{13} and was described process 13 by a simple linear first-order rate law. In our opinion, it would be desirable to study the single process of oxygen interphase transport and also to measure the time dependence of the dissolved oxygen concentration during the modified BR reaction. Nevertheless, computations for several different conditions have simulated experimental observations very satisfactorily. Therefore, it seems that the essential features of the mechanism of the Briggs–Rauscher oscillatory reaction with substrates containing active methylene hydrogens have been confirmed.

Finally, several new organic substrates have very recently been found³² to promote oscillations in batch conditions in the BR system. The new substrates, crotonic acid, acrylic acid, anisole, and *p*-nitrophenol, react with iodine (I) by either addition or substitution reactions. Some type of active reduction of HIO_2 to HOI must be included in the mechanism to allow for the simulation of oscillations with the new substrates.

Conclusion

Oscillations in the rate of gaseous oxygen production in the modified BR reaction with acetone were both observed experimentally and simulated using the NF model supplemented by the physical processes of iodine and oxygen interphase transport. Oscillations persist even at rapid stirring rates, and therefore, we do not expect that nucleation and supersaturation processes are major factors responsible for oscillatory behavior in the BR system. It was confirmed that the essential features of the mechanism of the BR oscillatory reaction with substrates that react via an enol mechanism could be properly explained on the basis of the Noyes and Furrow⁴ and De Kepper and Epstein⁵ models.

Acknowledgment. This work was supported by Grant 1/7301/20 from the Scientific Grant Agency of MESR.

References and Notes

- Briggs, T. S.; Rauscher, W. C. *J. Chem. Educ.* **1973**, *50*, 496.
- Epstein, I. R.; Pojman, J. A. *Introduction to Nonlinear Chemical Dynamics*; Oxford University Press: New York, 1998.
- Noyes, R. M. *J. Phys. Chem.* **1990**, *94*, 4404.
- Noyes, R. M.; Furrow, S. D. *J. Am. Chem. Soc.* **1982**, *104*, 45.
- De Kepper, P.; Epstein, I. R. *J. Am. Chem. Soc.* **1982**, *104*, 49.
- Cooke, D. O. *Int. J. Chem. Kinet.* **1980**, *12*, 683.
- Furrow, S. D. In *Oscillations and Traveling Waves in Chemical Systems*; Field, R. J., Burger, M., Eds.; Wiley-Interscience: New York, 1985 and references therein.
- Vanag, V. K.; Alfimov, M. V. *J. Phys. Chem.* **1993**, *97*, 1884.
- Melikhov, D. P.; Vanag, V. K. *Russian J. Phys. Chem.* **1995**, *69*, 1879.
- Kumpinsky, E.; Epstein, I. R.; De Kepper, P. *Int. J. Chem. Kinet.* **1985**, *17*, 345.
- Vukojević, V.; Sørensen, P. G.; Hynne, F. *J. Phys. Chem.* **1996**, *100*, 17175.
- Furrow, S. D.; Noyes, R. M. *J. Am. Chem. Soc.* **1982**, *104*, 42.
- Cervellati, R.; Mongiorgi, B. *Int. J. Chem. Kinet.* **1998**, *30*, 641.
- Cervellati, R.; Crespi-Perellino, N.; Furrow, S. D.; Minghetti, A. *Helv. Chim. Acta* **2000**, *83*, 3179.
- Nagy-Ungvarai, Z.; Müller, S. C.; Hess, B. *Chem. Phys. Lett.* **1989**, *156*, 433.
- Ševčík, P.; Kissimonová, K.; Adamčíková, L'. *J. Phys. Chem. A* **2000**, *104*, 3958.

- (17) Ševčík, P.; Adamčíková, L'. *J. Phys. Chem. A* **1998**, *102*, 1288.
- (18) Hindmarsh, A. C. In *Scientific Computing*; Stepleman, R. S., Ed.; North-Holland: Amsterdam, 1983.
- (19) Treindl, L'.; Noyes, R. M. *J. Phys. Chem.* **1993**, *97*, 11354.
- (20) Kissimonová, K.; Valent, I.; Adamčíková, L'.; Ševčík, P. *Chem. Phys. Lett.* **2001**, *341*, 345.
- (21) Láňová, B.; Vreštlál, J. *J. Phys. Chem. A* **2002**, *106*, 1228.
- (22) Furrow, S. D.; Noyes, R. M. *J. Am. Chem. Soc.* **1982**, *104*, 42.
- (23) Valent, I.; Adamčíková, L'.; Ševčík, P. *J. Phys. Chem. A* **1998**, *102*, 7576.
- (24) Schmitz, G. *J. Chim. Phys.* **1987**, *84*, 957.
- (25) Kolar-Anić, L.; Čupić, Ž.; Anić, S.; Schmitz, G. *J. Chem. Soc., Faraday Trans.* **1997**, *93*, 2147.
- (26) Rubin, M. B.; Noyes, R. M. *J. Phys. Chem.* **1987**, *91*, 4193.
- (27) Bowers, P. G.; Hoffstetter, Ch.; Letter, C. R.; Toomey, R. T. *J. Phys. Chem.* **1995**, *99*, 9632.
- (28) Bowers, P. G.; Bar-Eli, K.; Noyes, R. M. *J. Chem. Soc., Faraday Trans.* **1996**, *92*, 2843.
- (29) Wang, J.; Hynne, F.; Sørensen, P. G.; Nielsen, K. *J. Phys. Chem.* **1996**, *100*, 17593.
- (30) Noyes, R. M.; Rubin, M. B.; Bowers, P. G. *J. Phys. Chem.* **1992**, *96*, 1000.
- (31) Scheeline, A.; Kirkor, E. S.; Kovacs-Boerger, A. E.; Olson, D. L. *Mikrochim. Acta* **1995**, *118*, 1.
- (32) Furrow, S. D.; Cervellati, R.; Amadori, G. *J. Phys. Chem. A* **2002**, *106*, 5841.